Influence of stormwater infiltration systems on the structure and the activities of groundwater biofilms: Are the effects restricted to rainy periods?

Yohan Lebon, Simon Navel, Maylis Moro, Jérémy Voisin, Benoit Cournoyer, Clémentine François, Laurence Volatier, Florian Mermillod-Blondin

Title: Influence of stormwater infiltration systems on the structure and the activities of groundwater biofilms: are the effects restricted to rainy periods?table

Authors: Yohan Lebon[a,*], Simon Navel[a], Maylis Moro[a], Jérémy Voisin[a,b], Benoit Cournoyer[b], Clémentine François[a], Laurence Volatier[a], Florian Mermillod-Blondin[a]

[a] Univ Lyon, Université Claude Bernard Lyon 1, CNRS, ENTPE, UMR5023 LEHNA, F-69622, Villeurbanne, France

[b] Univ Lyon, UMR Ecologie Microbienne (LEM), Université Claude Bernard Lyon 1, CNRS 5557, INRA 1418, VetAgro Sup, 69680 Marcy L'Etoile, France.

* Corresponding author.

E-mail address: yohan.lebon@entpe.fr (Y. Lebon)

Abstract:

Stormwater infiltration systems (SIS) have been set up to collect and infiltrate urban stormwater runoff in order to reduce flooding and to artificially recharge aquifers. Such practices produce environmental changes in shallow groundwater ecosystems like an increase in organic matter concentrations that could drive changes in structure and functions of groundwater microbial communities. Previous works suggested that SIS influence groundwater physico-chemistry during either rainy and dry period but no study has examined the impact of SIS on groundwater microorganisms during both periods. This study aimed to fill this gap by assessing SIS impacts on groundwater quality parameters in three SIS with vadose zone thickness < 3 m during two contrasting meteorological conditions (rainy / dry periods). Physicochemical (dissolved organic carbon and nutrient concentrations) and microbial variables (biomass, dehydrogenase and hydrolytic activities, and bacterial community structure) were assessed on SIS-impacted and non-SIS-impacted zones of the aquifers for the three SIS. Using clay beads incubated in the aquifer to collect microbial biofilm, we show that SIS increased microbial activities, bacterial richness and diversity in groundwater biofilms during the rainy period but not during the dry period. In contrast, the significant differences in dissolved organic carbon and nutrient concentrations, biofilm biomass and bacterial community structures (Bray-Curtis distances, relative abundances of main bacterial orders) measured between SIS-impacted and non-SIS-impacted zones of the aquifer were comparable during the two periods. These results suggest

that structural indicators of biofilm like biomass were probably controlled by long-term effects of SIS on concentrations of dissolved organic matter and nutrients whereas biofilm activities and bacterial richness were temporally stimulated by stormwater runoff infiltrations during the rainy period. This decoupling between the structural and functional responses of groundwater biofilms to stormwater infiltration practices suggests that biofilms functions were highly reactive to fluxes associated with aquifer recharge events.

Keywords: infiltration basin, dissolved organic carbon, nutrient, microbial activity, biofilm structure, species sorting

1. Introduction

Modern human societies increasingly rely upon groundwater for agriculture, industry and drinking water supply. For example, almost 50 % of drinking water production in the world in 2010 was obtained from aquifers (van der Gun, 2012; Smith et al., 2016). This groundwater demand is expected to drastically increase in cities due to predicted urban growth. Indeed, urban water demand will increase by 80 % by 2050 (Flörke et al., 2018). In parallel with groundwater demand, growing urbanization and the associated expansion of impervious soil surfaces increase flooding risks in urban areas during rainy periods (Konrad, 2003) and limit natural groundwater recharge with stormwater (Pitt et al., 1999). In this context, stormwater infiltration systems (SIS) such as infiltration basins have been set up in urban areas to collect and infiltrate urban stormwater runoffs for reducing flooding risks and for recharging aquifers (Fletcher et al., 2015; Natarajan and Davis, 2015).

Stormwater infiltration practices through infiltration basins can cause environmental disturbances in groundwater ecosystems, such as significant inputs of contaminants like organic compounds and dissolved organic matter (DOM), temperature fluctuations over the seasons and sudden drops in electrical conductivity associated with infiltration of low-mineralized water (Barraud et al., 1999; Datry et al., 2004; Foulquier et al., 2009, 2010). Such disturbances have been shown to impact the structure and function of groundwater microbial communities and potentially alter their roles in organic matter processing and water purification processes (Griebler and Avramov, 2015; Voisin et al., 2018). Despite these roles of microbial communities in aquifers, studies examining the impact of SIS on groundwater microorganisms remain scarce but see (Foulquier et al., 2011; Barba et al., 2019; Colin et al., 2020).

The impacts of SIS on groundwater microorganisms largely depend on the ability of the unsaturated zone or vadose zone (VZ) to act as a buffer or filter against changes induced by stormwater infiltration (Fritch et al., 2000; Pabich et al., 2001; Foulquier et al., 2010; Voisin et al., 2020). Experiments conducted on the porous aquifer to the east of Lyon revealed significant effects of SIS on physicochemical conditions and groundwater microbiology in areas with thin (< 3 m) VZ, whereas moderate effects of SIS were observed in areas with thick (> 10m) VZ (Datry et al., 2005; Voisin et al., 2018; 2020). For SIS with thin VZ, enrichment in dissolved organic carbon (DOC) and increased microbial biomass, activities and bacterial diversity of biofilms were measured in groundwater zones impacted by recharge with stormwater runoff (Mermillod-Blondin et al., 2013). Based on this study, Voisin et al. (2018) hypothesized that

the effects of SIS on groundwater microbial communities during rainfall events could be due to (1) changes in physicochemical conditions -especially the enrichment of available OM- below SIS and/or (2) the transport of microorganisms from the soil and the VZ of SIS to groundwater during recharge with stormwater runoff.

These expectations suggest that the infiltration of stormwater runoff (i.e. during rainfall events) was the main mechanism explaining changes in physicochemical conditions and bacterial community structures following a rainfall event below SIS. Nevertheless, Datry et al. (2003) and Foulquier et al. (2010) observed higher DOC and orthophosphate concentrations in SIS-impacted groundwater than in non-SIS-impacted groundwater, even during dry periods. This long-term effect could be due to an accumulation of OM over time in SIS-impacted zones of the aquifer (Foulquier et al., 2010). These findings suggest that groundwater microbial communities may be influenced by physicochemical conditions induced by infiltration basins during rainfall events but also during dry periods. Consequently, comparisons of experiments performed during dry and rainy periods could be very informative to evaluate whether stormwater infiltration associated with rainfall events have short-term or long-term impacts on groundwater microorganisms.

The present study aims to compare the impacts of infiltration basins on groundwater microbiology during a rainy and a dry period. To assess these impacts of SIS, groundwater zones impacted by stormwater infiltration were compared to non-impacted ones considered as control zones. In situ experiments were done in three SIS with vadose zone thickness < 3 m during two meteorologically contrasted periods (i.e. rainy and dry). For each SIS, groundwater samples were collected using piezometers in SIS-impacted and non-SIS-impacted zones to evaluate physico-chemical changes due to stormwater infiltration. Clay beads incubated in these monitoring wells during rainy and dry periods were used as artificial substrates to sample and monitor groundwater biofilms (Mermillod-Blondin et al., 2019; Voisin et al., 2016, 2020).

Under the above hypothesis of a significant impact of stormwater infiltration on microorganisms, differences in biomass, activities and structure of the microbial biofilms developed on clay beads between SIS-impacted and non-SIS-impacted zones of the aquifer would be higher during a rainy period than during a dry period. The alternative hypothesis would be that the physicochemical conditions and especially DOC concentration in groundwater are long-term impacted by SIS, inducing comparable differences in microbial

communities between SIS-impacted and non-SIS-impacted zones of the aquifer during both rainy and dry periods.

2. Materials et Methods

2.1 Study sites

Field work was performed in three SIS located on the eastern aquifer of the Metropolitan area of Lyon characterized by highly permeable glacio-fluvial sediments (Supplementary Material 2; Foulquier et al., 2009; Voisin et al., 2020). These SIS were selected for their thin VZ (< 3 meters) and their long-term use by scientists and stakeholders for groundwater quality monitoring purposes **(**Datry et al., 2004; Foulquier, 2009). This selection was also made for covering a wide range of environmental conditions (infiltration surfaces of the basins, catchment areas and land use, Table 1). Each SIS is equipped with piezometer wells in their downstream and upstream zones, along the groundwater flow. These zones are further considered as SIS-impacted and non-SIS-impacted zones respectively, because groundwater flow may convey infiltrated stormwater effects only in the direction of the downstream zone.

2.2 Experimental design and sampling

Ten day *in situ* experiments were performed under two meteorological contrasted conditions: a rainy (September 2015) and a dry (September 2016) period. The rainy period was characterized by four significant rainfall events (peak > 5 mm/h) over the ten days with an accumulated rainfall of 112 mm (average over 5 piezometer) representing more than 80% of the accumulated rain over the month. Thus, the studied rainy period was particularly important in terms of accumulated rainfall, facilitating the detection of an impact of stormwater infiltration on groundwater bacterial communities.

The dry period consisted of a ten-day period preceded by more than 10 days of dry weather to prevent the short-term residual impacts of a previous rainfall event. For each meteorological condition (rainy/dry periods), groundwater microbiology and chemistry were determined at three SIS in upstream and downstream piezometer wells (respectively non-SIS-impacted and SIS-impacted zones). Three replicates of water and biofilm samples were collected for each zone of each SIS.

Expanded clay beads (clay beads having diameters between 7.1 and 9 mm and previously heated to 1,200 °C in a rotary kiln) were used as artificial substrates for sampling microbial communities in groundwater following previous studies (Voisin et al., 2016, 2020; Mermillod-Blondin et al., 2019). While several studies (Williamson et al., 2012; Zhou et al., 2012; Fillinger et al., 2018) have used natural substrates for sampling microbial communities in groundwater, use of artificial substrates does not lead to divergent results as biofilm growth and diversity measured on clay beads were comparable to those measured on natural gravel particles (Voisin et al., 2016). In each zone of each SIS, three nylon mesh bags (11.5x4.5 mm, 3.3 mm mesh size, Sefar Nitex 06-3300/59, Sefar AG, Heiden) containing thirty beads each were placed in piezometer wells (non-SIS-impacted/SIS-impacted) for an incubation of ten days. This incubation time of 10 days was based on previous laboratory and field experiments (Voisin et al. 2016, 2020; Mermillod-Blondin et al. 2019) to obtain (1) a significant microbial colonization of clay beads in groundwaters and (2) a time-integrated monitoring of micro-organisms from impacted and non-impacted zones of the aquifer. After retrieval, the thirty beads from each bag were randomly split into four subsets dedicated to the evaluation of microbial characteristics (i.e. biomass; hydrolytic activity; dehydrogenase activity; bacterial community structure). As clay beads from each bag were used to measure all microbial variables, mean biofilm parameters per zone were calculated from three values (corresponding to batches of clay beads from the three bags incubated in the same zone). In addition to clay bead incubation, groundwater was sampled in the same wells using the Bou-Rouch method (Bou and Rouch, 1967) at three times for both rainy and dry periods to evaluate physico-chemical impacted associated with SIS: just before (T = 0 day), during (T = 5 days) and just after (T = 10 days) incubation of clay beads in groundwater.

2.3 Physicochemical analyses

Groundwater samples were filtered (0.7 µm pore size Whatman™ GF/F filters, GE Healthcare, Boston, MA, USA) to remove particles. Ammonium ($N\text{-}NH_4^+$), nitrate and nitrite (called $N\text{-}NO_3^-$ thereafter because $N\text{-}NO_2^-$ concentrations were negligible compared with $N\text{-}NO_3^-$ concentrations), and orthophosphate ($P\text{-}PO_4^{3-}$) concentrations were measured following standard colorimetric methods, using an automatic analyzer (Smartchem 200, AMS Alliance, Roma, Italy). DOC concentration was measured with a total carbon analyzer (multi-N/C 3100, Analytik Jena, Jena, Germany) based on sample combustion at 900°C and CO_2 stripping under O_2 flow, after removal of dissolved inorganic C with hydrochloric acid (250 µL HCl 35 %).

2.4 Microbial analyses

2.4.1 Microbial biomass

Biomass of microbial biofilm developed on clay beads was assessed by the quantification of total protein content (Sigma Protein Assay Kit P-5656, Sigma-Aldrich, St Louis, MO, USA), using the method of Peterson (1977) and following the protocol described in Voisin et al. (2020). Five beads were treated with 2 mL of ultrapure water and 2 mL of Lowry's reagent for 20 minutes under stirring to improve contacts between Lowry's reagent and biofilm-related proteins. Color reaction started with the addition of 0.5 mL of Folin reagent and developed for 30 minutes. Final solution was filtered (0.7 µm pore size Whatman^{TM} GF/F filters, GE Healthcare, Boston, MA, US) to remove particles before measuring its optical density at 750 nm in a 1-cm thick cuvette with a spectrophotometer (Aquamate, ThermoSpectronic, Cambridge, GB). Conversion of measured optical densities to total protein biomass was realized using a calibration line obtained with BSA (bovine serum albumin lyophilized powder ≥ 96 %, Sigma-Aldrich, St Louis, MO, US). Protein biomass was then expressed in µg per surface of clay bead in cm^2 (calculated from the dry weight of the subset of five beads used for the analysis and a pre-calculated mean value for the relationship between the surface and the density of clay beads) and corrected by results obtained for controls (sets of five sterile beads).

2.4.2 Microbial activities

Hydrolytic activity of microbial communities was estimated using the fluorescein diacetate (3,6-diacetyl-fluorescein; FDA) hydrolysis method (Fontvieille et al., 1992). Beads were incubated with 3 mL of a pH 7.6 phosphate buffer solution for 40 minutes to stabilize the temperature before incubation. Coloration step then started by adding 0.1 mL of FDA solution (10 mg of FDA diluted in 6 mL of acetone and 4 mL of ultrapure water) in vials stored in the dark at 15ºC. During this step, colorless FDA is hydrolyzed by non-specific extracellular and membrane-bound enzymes to produce green fluorescein. Incubation was ended with the addition of 3 mL acetone when green coloration was visible (after 18-24 hours). Final supernatant was filtered (0.7 µm pore size Whatman^{TM} GF/F filters, GE Healthcare, Boston, MA, USA) to remove particles before measuring its optical density at 490 nm in a 1-cm thick

cuvette with a spectrophotometer (Aquamate, ThermoSpectronic, Cambridge, UK). Hydrolytic activity is then calculated following the equation:

Hydrolytic activity = (OD_{490} * 6.1) / (81.3 * t * S)

where hydrolytic activity is expressed in quantity of FDA hydrolyzed per hour and cm^2 of clay bead surface (µmol FDA $.h^{-1}.cm^{-2}$), OD_{490} is the optical density measured at 490 nm (cm^{-1}), 6.1 is the volume of dilution (in mL), 81.3 is the molar extinction coefficient of fluorescein (µmol $.mL^{-1}.cm^{-1}$), t is the incubation time (in h) and S is the total surface of the 5 clay beads used for the analysis (in cm^2). In the same way as for microbial biomass analyses, the quantity of FDA hydrolyzed per hour (i.e. hydrolytic activity) was corrected by results obtained from controls (sterile clay beads).

Dehydrogenase activity of microbial communities was estimated through measurements of 2-(4-iodophenyl)-3-(4-nitrophenyl)-5-phenyl tetrazolium chloride (INT) to INT-formazan reduction rates (Houri-Davignon et al., 1989). Five beads were first incubated with 0.1 mL INT solution (2 % in methanol) and 4 mL filtered water (0.2 µm pore size Whatman™ nuclepore polycarbonate track-etched membrane, GE Healthcare, Boston, MA, USA) from the corresponding piezometer, in the dark at 15°C for incubation times similar to those performed for hydrolytic activity analyses (between 18 and 24 hours). The incubation was stopped by adding 0.5 mL of formol at 37 %. During this incubation, colorless INT is gradually reduced by electron transport system (ETS) and the resulting optically dense formazan is accumulating in cells. Then, we replaced the supernatant with 4 mL methanol to start a 12 hour-long extraction of INT-formazan. To ensure the collection of all microorganisms and a complete extraction, i) the supernatant was filtered with 0.2 µm pore size membrane (Whatman™ nuclepore polycarbonate track-etched membrane, GE Healthcare, Boston, MA, USA) to collect free microbial cells present in the supernatant; ii) the filter was put in the glass flask containing the clay beads and methanol was added to the flask for starting INT-formazan extraction; iii) a 2-min sonication was applied to enhance the action of methanol on microorganisms (developed on beads or retained on the membrane). Final supernatant was filtered (0.7 µm pore-size Whatman™ GF/F filters, GE Healthcare, Boston, MA, USA) to remove particles before measuring its optical density at 480 nm in a 1-cm thick cuvette with a spectrophotometer (Aquamate, ThermoSpectronic, Cambridge, GB). Dehydrogenase activity is then calculated following the equation:

Dehydrogenase activity = (OD_{480} * 4) / (18 * t * S)

where dehydrogenase activity is expressed in quantity of INT hydrolysed per hour and cm^2 of clay bead surface (µmol INT $.h^{-1}.cm^{-2}$), OD_{480} is the optical density measured at 480 nm (cm^{-1}), 4 is the volume of dilution (in mL), 18 is the molar extinction coefficient of INT in methanol ($mL.\mu mol^{-1}.cm^{-1}$), t is the incubation time (h), and S is the total surface of the five clay beads used for the analysis (in cm^2). Here again, the quantity of INT-formazan produced per hour (i.e. dehydrogenase activity) was corrected by results obtained from controls (sterile clay beads).

2.4.3 Bacterial community structure

For each sample, we retrieved microbial cells by shaking (2 minutes at 2500 rpm using a vortex) fifteen clay beads in 10 mL 0.8 % NaCl and then filtered the suspended cells on a 0.2 µm pore size membrane (Whatman™ nuclepore polycarbonate track-etched membrane, GE Healthcare, Boston, MA, USA). DNA extraction of cells collected on membranes was realized using FastDNA™ Spin Kit for Soil (MP Biomedicals, Irvine, CA, USA). The amount of extracted DNA was quantified using a Nanodrop ND1000 spectrophotometer (Thermo Fisher Scientific, USA).

The V5-V7 region of the 16S gene was amplified using the 799F (5'-AACMGGATTAGATACCCKG; Beckers et al., 2016) and bac1193R (5'-CRTCCMCACCTTCCTC; Maes et al., 2016) primers. All samples were sequenced on an Illumina Miseq platform (paired-end reads 2 * 300 bp) at MR DNA (Shallowater, TX, USA).

Bioinformatic processing of the merged 2x300 bp paired-end reads followed sequential steps: 1) dereplication and filtering (keeping only 300 to 500 bp –long reads containing a valid mismatch-free tag and no ambiguous base), 2) clustering into operational taxonomic units (OTUs) with SWARM (Mahé et al., 2014; two-step-procedure: local clustering threshold d=1 and then d=3), 3) removal of chimera, 4) removal of OTUs detected in only one out of three replicates from same condition, 5) abundance normalization (by rarefaction, i.e. subsampling at 50,233 reads per sample, to correct for variability in sequencing depths among samples) and 6) taxonomic affiliation against the 16S SILVA database release 132 (Quast et al., 2012), based on NCBI blastn+ (Altschul et al, 1990) and allowing for multiple affiliation. These different steps were performed within FROGS (Find Rapidly OTUs with Galaxy Solution, Escudié et al., 2018) except for step 4) realized with R version 3.5.1 (R Core Team, 2018).

Seed sequences representing each OTUs were then aligned ("AlignSeqs" function from the R package "DECIPHER" version 2.10.1; Wright, 2016) and gaps (position in the alignment with ≥1 % of aligned seed sequences missing the base information) were removed ("deleteGaps" function from the R package "ips" version 0.0-7; Heibl, 2008). Quality of alignment was visually checked (using SeaView, Gouy et al., 2010) prior to the construction of an optimized GTR+G+I maximum likelihood tree (built with a neighbor-joining tree as starting point). Tree was constructed by using the R packages "ape" version 5.2 (Paradis and Schliep, 2019) and "phangorn" version 2.4.0 ("NJ" and "pml" functions, Schliep, 2011**)**.

At the community scale, alpha diversity was evaluated through the OTUs richness (function "specnumber" from the R package "phyloseq" version 1.24.2, (McMurdie and Holmes, 2013)), the Shannon diversity index (function "diversity" from the same package) and the Faith's phylogenetic diversity index (function "pd" from the R package "picante" version 1.8 package, Kembel and Kembel, 2019).

Beta diversity (i.e. differences in bacterial composition between two communities) was evaluated with Bray-Curtis and weighted unifrac distances (Lozupone and Knight, 2005) (function "distance" from R package phyloseq version 1.24.2, McMurdie and Holmes, 2013). These distances were calculated between non-SIS-impacted and SIS-impacted zones for each SIS. As three bacterial community compositions (triplicates) were determined per zone and SIS, mean distances per SIS were obtained by averaging the nine pairwise distances calculated between each non-SIS-impacted community and each SIS-impacted community (three non-SIS-impacted communities * three SIS-impacted communities = nine pairwise distances). For the calculation of weighted unifrac distances, the optimized GTR+G+I tree obtained previously was midpoint rooted using the function "midpoint" from the R package "phangorn".

2.5 Data deposition

Sequence data are available at the European Nucleotide Archive (https://www.ebi.ac.uk/ena) under the project accession numbers #PRJEB29925 and #PRJEB40243. See Table S2 for barcode information.

2.6 Data analyses

The effects of the position ("impacted zone" and "non-impacted zone") and the meteorological condition ("dry period" and "rainy period") on chemical and microbiological variables (mean values from the three replicated bags per zone and well) were tested using repeated-measure analyses of variance (two-way RM-ANOVA) with period as fixed factor and position as repeated factor to take into account the non-independence of impacted and non-impacted wells in each SIS. Our main hypothesis being an increased effect of the position during the rainy period, we focused on the statistical interaction between "position" and "period" in statistical tests. All data were √-transformed to satisfy the normality assumption verified by Shapiro's test. Sphericity assumption for RM-ANOVA was verified using Mauchly's sphericity test. Dissimilarities in bacterial communities between SIS impacted and non-SIS-impacted zones were calculated for each SIS and period using Bray-Curtis and unnormalized weighted Unifrac distances. Values for Bray-Curtis and Unifrac distances were √-transformed and compared using a one-way ANOVA (with period as main factor).

Based on taxonomic affiliations, we tested the influences of the position and period on the relative abundances of the ten most abundant bacterial orders (representing more than 95 % of the total number of reads) in bacterial communities using a repeated-measure analyses of variance (two-way RM-ANOVA) with period as fixed factor and position as repeated factor . This analysis has been done after a √-transformation of the dataset (as done for other variables). All statistical tests were performed using the R software (R Core Team, 2018).

3. Results

3.1. Groundwater physico-chemistry

For the three SIS (i.e. MIN, GB and IUT), high similarities in physico-chemical conditions were measured during the dry and the rainy periods (Fig. 1A for DOC concentration and Table S1), with comparable patterns between SIS-impacted and non-SIS-impacted zones. Indeed, DOC concentrations were significantly higher in SIS-impacted than in non-SIS-impacted zones, during both rainy and dry periods (Fig. 1A, two-way RM-ANOVA, "position" effect, $p < 0.01$). Considering the two periods, average DOC concentration values were 2.1-fold, 1.7-fold and 2.2-fold higher in SIS-impacted than in non-SIS-impacted zones for MIN, GB and IUT, respectively. The same trends were observed for $N\text{-}NH_4^+$ and $P\text{-}PO_4^{3-}$ concentrations with higher values in SIS-impacted zones, although no significant statistical results were obtained due to the high variability among SIS (two-way RM-ANOVA, position effect, $0.11 > p > 0.05$ for these two variables). The inverse pattern was observed for $N\text{-}NO_3^-$ concentrations with

values which tended to be lower in SIS-impacted than in non-SIS-impacted zones (Table S1, two-way RM-ANOVA, position effect, $0.1 > p > 0.05$). Although a significant effect of the period (rainy vs. dry) was detected on DOC concentrations (Fig. 1A and Table S1, two-way RM-ANOVA mixed model, "period" effect, $p < 0.05$), the differences in DOC, P-PO_4^{3-}, N-NH_4^+ and N-NO_3^- concentrations measured between SIS-impacted and non-SIS-impacted zones were not significantly influenced by the period (two-way RM-ANOVA, interaction between "position" and "period" effects, $p > 0.3$ for all variables).

3.2. Microbial biomass and activities

As observed for DOC concentrations, significantly higher total protein contents per cm^2 of clay beads (considered as a proxy for microbial biomass) were detected in SIS-impacted than in non-SIS-impacted zones for the three SIS, during both rainy and dry periods at the unique exception of the GB SIS during the dry period (Fig. 1B, two-way RM-ANOVA, "position" effect, $p < 0.05$, interaction between "position" and "period" effects, $p > 0.4$). For example, microbial biomasses in IUT SIS . (Fig. 1B).

In contrast with microbial biomass patterns, dehydrogenase activity of the biofilm was only significantly higher in SIS-impacted zones than in non-SIS-impacted zones during the rainy period (Fig. 1C, two-way RM-ANOVA, interaction between "position" and "period" effects, $p < 0.05$). The same trend was observed for hydrolytic activity although statistical tests were not significant with $\alpha = 5\%$ (Fig. 1D, two-way RM-ANOVA, interaction between "position" and "period" effects, $0.10 > p > 0.05$). For example, biofilms developed in SIS-impacted zone of GB site exhibited a 3-fold higher hydrolytic activity than biofilms developed in non-SIS-impacted zone of GB during the rainy period whereas hydrolytic activities were comparable between the SIS-impacted and the non-SIS-impacted zones of GB site during the dry period (Fig. 1D).

3.3. Analyses of biofilm bacterial community structures

The sequencing of the 16S rRNA V5-V7 libraries yielded high-quality sequences distributed across 36 biofilm samples. After rarefaction-based abundance normalization (subsampling 50,233 sequences per sample), all sequences were clustered into 7,600 OTUs with the algorithm SWARM (in FROGS).

OTUs richness (i.e. number of OTUs present in a given sample) was significantly higher in SIS-impacted zones in comparison with non-SIS-impacted zones at both periods (Fig. 2, two-

way RM-ANOVA, "position" effect, $p < 0.05$). Although no significant interaction between position and period effects due to the variability among SIS (two-way RM-ANOVA, interaction between "position" and "period" effects, $0.11 > p > 0.05$), differences in OTUs richness (i.e. number of OTUs present in a given sample) between SIS-impacted and non-SIS impacted zones were lower during the dry period (mean increase of 26% in OTUs numbers per SIS) than during the rainy period (mean increase of 91% in OTUs numbers per SIS) (Fig. 2). These trends in OTUs richness were in line with those observed from the computing of relative abundances of OTUs (Shannon index) and of their phylogenetic relationships (Phylogenetic index) (Fig. 2).

In each SIS, the biofilm groundwater bacterial richness in SIS-impacted and in non-SIS-impacted zones was predominantly associated with OTUs specifically found in each zone because less than 32 % of OTUs (maximum percentage corresponding to IUT SIS in dry period) were shared between these two zones (Fig. 3). For the three SIS, the percentages of OTUs shared between non-SIS-impacted and SIS-impacted zones (Fig. 3) were not higher during dry period (24-32 %) than during rainy period (18-30 %). These shared OTUs included the most abundant ones as they represented between 92.1 and 97.7 % of the reads in the dataset (for the two periods; see Fig3). Indeed, the sixteen most abundant OTUs out of the 7,600 OTUs in the dataset (i.e. 0.2 % of the total OTUs) represented 50 % of total reads (Supplementary material 1). Then, the higher difference in OTUs richness between SIS-impacted zones and non-SIS-impacted zones in rainy period compared to the dry period (Fig. 2) was due to a higher number of OTUs that were not numerically dominant in the dataset. These OTUs represented in average 56 % of total OTUs number but only 4.4 % of reads (Fig. 3).

We did not detect any effect of the period (rainy vs dry) on the dissimilarity of bacterial community profiles from SIS-impacted and non-SIS-impacted zones, when assessed with Bray-Curtis distances (Fig. 4, one-way ANOVA, "period" effect, $p > 0.6$).

The same results were obtained when phylogenetic distances were considered using the weighted UNIFRAC unnormalized distances (Fig. 4, one-way ANOVA, "period" effect, $p > 0.2$), indicating that bacterial community structures were not more divergent between SIS-impacted and non-SIS-impacted zones during the rainy than during the dry period.

Whatever the SIS and the period considered, the Bray-Curtis and weighted UNIFRAC unnormalized dissimilarities calculated between the bacterial communities in the SIS-impacted and in the non-SIS-impacted zones were always higher than 0.46 (Fig. 4).

3.4. Bacterial taxonomic affiliations from aquifer biofilms

Bacterial taxa of aquifer biofilms developing on artificial substrates (clay beads) and inferred from the 16S rRNA V5-V7 dataset were dominated by *Beta-proteobacteriales* (43.5 % of reads in the dataset) and *Pseudomonadales* (21.5 % of reads), two orders of Gamma-proteobacteria (Fig. 5). Gene reads from the *Flavobacteriales* (Bacteroidia) were also detected in SIS-impacted and non-SIS-impacted zones of all SIS but with lower relative abundances (12.7 % of reads) than those allocated to the *Beta-proteobacteriales* and *Pseudomonadales*.

Although the proportion of gene reads from the *Beta-proteobacteriales* (Gammaproteobacteria) did not vary significantly with the position (non-SIS-impacted/SIS-impacted zones) (two-way RM-ANOVA, "position" effect, $p > 0.96$), the proportion of reads from the *Pseudomonadales* (Gammaproteobacteria) in the biofilms was lower in SIS-impacted zones comparing to non-SIS-impacted zones, during both dry and rainy periods (Fig. 5, two-way RM-ANOVA, "position" effect, $p < 0.01$). These lower proportions of reads from the *Pseudomonadales* in SIS-impacted zones of GB and IUT were mainly associated with increased proportions of reads from the *Flavobacteriales* (Bacteroidia). A different pattern was observed in MIN with increased proportion of reads from the *Alteromonadales* (Gamma-proteobacteria) during the dry period and increased proportion from the *Rhodobacterales* (Alpha-proteobacteria) during the rainy period in SIS-impacted zone (Fig. 5). V5-V7 reads from the *Clostridiales* (Clostridia) and *Micrococcales* (Actinobacteria) also contributed significantly to the dataset (> 1.2 % of reads for each taxon) but they were restricted to one zone of one SIS at one period: (i) reads from the *Clostridiales* (Clostridia) in the SIS-impacted zone of GB during the dry period, and (ii) reads from the *Micrococcales* (Actinobacteria) in the SIS-impacted zone of IUT during the rainy period (Fig. 5).

4. Discussion

The present results confirmed the long-term influences of SIS on groundwater chemistry reported in previous studies (Datry et al., 2004; Foulquier et al., 2010): higher DOC, $P\text{-}PO_4^{3-}$ and NH_4^+ concentrations were measured in SIS-impacted groundwater than in non-SIS-impacted groundwater during both rainy and dry periods. NO_3^- concentrations were also lower in SIS-impacted than in non-SIS-impacted zones of the aquifer during both rainy and dry periods. These results indicate that SIS impact on groundwater chemistry was not only driven

by the transfer of water, organic matter and nutrients with stormwater infiltration. For example, decreased concentrations of $N\text{-}NO_3^-$ in SIS-impacted zones of the aquifer in comparison with non-SIS-impacted zones were often explained by a dilution of groundwater $N\text{-}NO_3^-$ concentrations with infiltrated stormwater poor in $N\text{-}NO_3^-$ (Foulquier et al. 2010, Mermillod-Blondin et al. 2013). In this situation, we can hypothesize that stimulation of biogeochemical processes like denitrification in aquifer zones impacted by SIS might explain the lower concentrations of $N\text{-}NO_3^-$ measured in SIS-impacted zones than in non-SIS-impacted zones of the aquifer during dry periods. This denitrification hypothesis seems very plausible because SIS-impacted zones were characterized by more favorable conditions for denitrification processes (higher DOC concentrations and lower dissolved oxygen concentrations, Table S1) than non-SIS impacted zones. This long-term effect (during both dry and rainy periods) of the SIS on NO_3^- concentrations but also on NH_4^+, PO_4^{3-} and DOC concentrations could be due to the accumulation of organic matter in sediment below SIS observed by Foulquier et al. (2010) in the same SIS. For example, these authors measured an enrichment of more than 50 % in content of sedimentary organic carbon in SIS-impacted zone (around 310 mg C per kg of dry sediment in the top 30 cm below the groundwater table) of IUT SIS than in non-SIS-impacted zone of the same SIS (around 200 mg C per kg of dry sediment in the top 30 cm below the groundwater table). Sedimentary organic matter enrichment in the aquifer may then act as a source of DOC and nutrients like PO_4^{3-} and NH_4^+ but also as a zone of denitrification (as observed in slow filtration columns by Nogaro et al., 2007). Consequently, accumulation of sedimentary organic matter below SIS might have led to dissolved oxygen and NO_3^- reductions (Table S1), and NH_4^+, PO_4^{3-} and DOC releases and enrichments in SIS-impacted zones compared to non-SIS-impacted zones of the aquifer whatever the period.

Following these long-term effects of SIS on groundwater chemistry, differences in biofilm biomass between the SIS-impacted and non-SIS-impacted zones of the aquifer were also comparable during the rainy and dry periods. Dissimilarities in bacterial community structures between SIS-impacted and non-SIS-impacted zones were relatively high at the two periods ($d > 0.46$, Figure 4) and were more likely linked to comparable differences in the main proportions of bacterial orders between zones (Figure 5). These latter results suggest that both biofilm biomass and bacterial community structures were associated with long-term effects of the SIS on groundwater chemistry. DOC being the main limiting compound for microbial growth in most aquifers (Bengtsson, 1989; Starr and Gillham, 1993; Goldscheider et al., 2006; Mermillod-Blondin et al., 2013), its enrichment increased the carrying capacity of the system in terms of

microbial biomass (Rauch-Williams and Drewes, 2006; Williamson et al., 2012; Li et al., 2013) and played a key role on bacterial community structures (as shown in other ecosystems, (Findlay et al., 2003; Li et al., 2012), which is consistent with the results of this study.

The bacterial community analyses showed a decrease in relative abundances of *Pseudomonadales* (essentially *Pseudomonas* sp. > 93 %) in SIS-impacted zones (enriched in DOC) in comparison with non-SIS-impacted zones. Such result could be due to the influence of DOC and nutrient availability on bacterial community structure of biofilms (Miura et al., 2015; Muscarella et al., 2019), *Pseudomonadales* being potentially less competitive than other bacterial groups when organic carbon availability increased in the aquifer. This hypothesis is consistent with our results showing that the impoverishment in relative abundances of *Pseudomonadales* was associated with an enrichment in *Flavobacteriales* in SIS-impacted zones in comparison with non-SIS-impacted zones of the aquifer for IUT et GB SIS. Indeed, members of the *Flavobacteriales* order are often abundant in nutrient-rich aquatic environments (Cho and Kim, 2000; Fandino et al., 2005; Marti et al., 2017; Voisin et al., 2020) and might have been favored in bacterial communities of SIS-impacted zones of the aquifer enriched in DOC. For MIN SIS, this impoverishment in relative abundances of *Pseudomonadales* in SIS-impacted zones in comparison with non-SIS-impacted zones was associated with an enrichment in relative abundances of *Alteromonadales* (essentially *Rheinheimera* > 99.6 % of all orders) in the dry period and *Rhodobacterales* (essentially *Rhodobacter* > 62 % of *Rhodobacterales* in MIN SIS) in rainy period. As observed for *Flavobacteriales*, this enrichment suggested that the members of these two groups were more competitive than *Pseudomonadales* in nutrient-rich environments (Brettar, 2006; He et al., 2019; Kumar et al., 2015). However, more specific analyses are required to validate this hypothesis that competition between *Pseudomonadales* and other bacterial groups depends on C availability in the environment. Firstly, the 16S rRNA gene (used in this study) is generally not reliable enough for taxonomic allocations at the species level. Other metabarcoding markers are also required (e.g. *tpm* in Colin et al., 2020) to investigate competition at the species and sub-species taxonomic levels. In addition, some hypotheses for explaining trends among these biofilm bacterial communities from SIS-impacted and non-SIS-impacted groundwaters could be experimentally tested by laboratory experimentations using groundwater with contrasting DOC concentrations. Monitoring changes in bacterial community structures during the experiments would be very pertinent to determine whether C availability drives species/strains sorting towards *Flavobacteriales* or other bacterial groups.

Results of biofilm biomass and bacterial community structure support the hypothesis stating that physicochemical conditions and especially DOC concentration in groundwater are long-term impacted by SIS, inducing comparable differences in microbial communities between SIS-impacted and non-SIS-impacted zones of the aquifer during both rainy and dry periods. However, microbial activities and bacterial diversity of the biofilm gave contrasting results and supported the hypothesis that the influence of SIS on groundwater biofilms significantly depend upon meteorological conditions (rainfall events and stormwater infiltration). Indeed, microbial activities were largely modulated by meteorological conditions as increases in microbial activities in the SIS-impacted zones compared to the non-SIS-impacted zones were only observed during the rainy period. These results contrasted with previous studies (Mermillod-Blondin et al., 2013; Voisin et al., 2019b) showing a correlation between biomass and activities of groundwater biofilms. In the present study, microbial activities were not correlated with microbial biomass during the dry period: microbial biomass was significantly higher in SIS-impacted zone than in non-SIS-impacted zones whereas microbial activities were not significantly different between zones. Such disconnection between biomass and activity has been already reported in literature (Moorhead et al., 2013; Rinkes et al., 2013; Hofmann and Griebler, 2018). For example, Moorhead et al. (2013) showed that the equilibrium between enzymatic activities and microbial biomass could be highly disconnected due to differences in the availability of nutrients in soil mesocosms (enzymatic activities being dependent on the concentration of available substrates). In the present study, rainy conditions enhanced the water flow in the SIS-impacted zones of the aquifer and then increased available DOC and phosphorus (PO_4^{3-}) fluxes supplied to the groundwater biofilm, stimulating its activity and its biomass (Mermillod-Blondin et al., 2013). The stimulation of microbial activity and biomass with hydrological fluxes has been already demonstrated in sedimentary environments (Battin, 2000; Mentzer et al., 2006; Foulquier et al., 2011; Freimann et al., 2015**)**. In contrast, DOC enrichments in SIS-impacted zones during dry period did not influence similarly bacterial biomass and activities: biomass was significantly higher in SIS-impacted than in non-SIS-impacted zones whereas no difference between zones were detected for microbial activities. In these conditions, we can hypothesize that fluxes of water, DOC and PO_4^{3-} associated with stormwater infiltration during rainy period fed the whole biofilm biomass whereas all the biomass of the biofilm did not have access to available DOC and PO_4^{3-} concentrations under low-flow condition (dry period without stormwater infiltration). Supporting this hypothesis, Battin and Sengschmitt (1999) showed inverse responses of biofilm biomass and esterase activity to flow conditions in streambed sediments. They demonstrated that esterase activity

was inhibited when low water flow conditions and extra-polymeric substances associated with biofilm biomass limited the supply of organic compounds to bacterial cells. Consequently, biofilm functioning might have been largely controlled by DOC and water fluxes, regulating metabolic pathways between anabolism (associated with biomass production) and catabolism (associated with physiological activities) (Grösbacher et al., 2018; Carlson et al., 2007; Liu et al., 2003; Liu and Tay, 2001).

As observed for microbial activities, bacterial richness and diversity were higher in biofilms from SIS-impacted zones than in biofilms from non-SIS-impacted zones only during the rainy period. This influence of rainy conditions might have been due to a temporary increased water flow below SIS that favored the transport of surface bacteria into the groundwater system (SIS-impacted zone) and/or the remobilization of bacterial taxa living at the vadose zone - groundwater interface (Smith et al., 2018; Voisin et al., 2018). Another phenomenon could also explain the increased bacterial richness and diversity associated with rainy conditions: mobilization of organic matter in the vadose zone during stormwater infiltration in the rainy period might have enhanced the diversity of organic compounds present in groundwater, supporting a more diverse community of bacteria in the aquifer (Flynn et al., 2013; Landa et al., 2013). At this stage, more experiments (e.g., complete analysis of the diversity of organic compounds in DOC, (Her et al., 2003; Seitzinger et al., 2005) are needed to evaluate the respective influences of trophic conditions and bacterial transfers on bacterial diversity changes observed below SIS. Nevertheless, it is worth noting that bacterial diversity changes were not associated with changes in very abundant OTUs (see Figure 3). Indeed, in rainy period, the OTUs specific to the impacted zones represented in average 56 % of all OTUs, but only 4.4 % of the reads in the metabarcoding dataset. This observation does not mean that low relative abundance of taxa cannot be important in terms of biogeochemical or health issues, but these issues need more specific analyses (qPCR on genes targeting specific pathogenic bacteria or functions, Cavalca et al., 2004; Winderl et al., 2007) which are out of the scope of the present paper.

In summary, differences in biofilm structure (biomass, bacterial community structure) between SIS-impacted and non-SIS-impacted zones of the aquifer were observed during both dry and rainy periods and could be attributed to a long-term effect of the SIS, potentially through an accumulation of organic matter in the top sedimentary layer below the groundwater table. In contrast, biofilm activities were largely influenced by meteorological conditions with higher

microbial activities in SIS-impacted than in non-SIS-impacted zones during the rainy period suggesting that groundwater biofilms are able to rapidly respond to environmental changes associated with stormwater infiltration. Nevertheless, the present analysis only focused on two periods of 10 days with their specific meteorological characteristics including very strong stormwater events (as indicated in the material and methods). Thus, expanding the present study to multiple rainfall events of different intensities is needed to obtain a more complete view of the sensitivity of groundwater microbial activities to varying hydrological conditions. In addition, as changes in groundwater microbial communities can occur from months to years (Zhou et al., 2012; Fillinger et al., 2018; Herzyk et al., 2017), the long-term dynamics of microbial communities should be integrated in future studies to assess the consequences of stormwater infiltration on groundwater ecosystems.

Acknowledgements: The authors thank Antonin Vienney, Félix Vallier, Edwige Gautreau and Pierre Marmonier for their assistance and advice during field and laboratory work.

Funding: This work was supported by l'Agence Nationale de la Recherche [ANR-16-CE32-0006 FROG], Lyon Metropole and Agence de l'Eau Rhône-Méditerranée-Corse within the framework of the experimental observatory for urban hydrology (OTHU, http://www.graie.org/othu/) and Rhône Basin LTER (ZABR). The authors also thank the Auvergne-Rhône-Alpes region for Jérémy Voisin's Ph.D grant. This work was performed within the framework of the EUR H2O'Lyon (ANR-17-EURE-0018) of Université de Lyon (UdL), within the program "Investissements d'Avenir" operated by the French National Research Agency (ANR).

References

Altschul, S. F., Gish, W., Miller, W., Myers, E. W., & Lipman, D. J., 1990. Basic local alignment search tool. Journal of molecular biology, 215(3), 403-410. https://doi.org/10.1016/S0022-2836(05)80360-2

Barba, C., Folch, A., Sanchez-Vila, X., Martínez-Alonso, M., Gaju, N., 2019. Are dominant microbial sub-surface communities affected by water quality and soil characteristics? J. Environ. Manage. 237, 332–343. https://doi.org/10.1016/j.jenvman.2019.02.079

Barraud, S., Gautier, A., Bardin, J.-P., Riou, V., 1999. The impact of intentional stormwater infiltration on soil and groundwater. Water Sci. Technol. 39, 185. https://doi.org/10.1016/S0273-1223(99)00022-0

Battin, T.J., 2000. Hydrodynamics is a major determinant of streambed biofilm activity: From the sediment to the reach scale. Limnol. Oceanogr. 45, 1308–1319. https://doi.org/10.4319/lo.2000.45.6.1308

Battin TJ., Sengschmitt D., 1999. Linking sediment biofilms, hydrodynamics, and river bed clogging: evidence from a large river. Microb Ecol. 37(3),185-196. doi:10.1007/s002489900142

Beckers, B., Op De Beeck, M., Thijs, S., Truyens, S., Weyens, N., Boerjan, W., Vangronsveld, J., 2016. Performance of 16s rDNA primer pairs in the study of rhizosphere and endosphere bacterial microbiomes in metabarcoding studies. Front. Microbiol. 7, 650. https://doi.org/10.3389/fmicb.2016.00650

Bengtsson, G., 1989. Growth and metabolic flexibility in groundwater bacteria. Microb. Ecol. 18, 235–248. https://doi.org/10.1007/BF02075811

Bou, C., Rouch, R., 1967. Un nouveau champ de recherches sur la faune aquatique souterraine. CR Acad Sci 265, 369–370.

Brettar, I., 2006. Rheinheimera perlucida sp. nov., a marine bacterium of the Gammaproteobacteria isolated from surface water of the central Baltic Sea. Int. J. Syst. Evol. Microbiol. 56, 2177–2183. https://doi.org/10.1099/ijs.0.64172-0

Carlson, C.A., Del Giorgio, P.A., Herndl, G.J., 2007. Microbes and the dissipation of energy and respiration: from cells to ecosystems. Oceanography 20, 89–100. https://doi.org/10.5670/oceanog.2007.52

Cavalca, L., Dell'Amico, E., Andreoni, V., 2004. Intrinsic bioremediability of an aromatic hydrocarbon-polluted groundwater: diversity of bacterial population and toluene monoxygenase genes. Appl. Microbiol. Biotechnol. 64, 576–587. https://doi.org/10.1007/s00253-003-1449-6

Cho, J.-C., Kim, S.-J., 2000. Increase in bacterial community diversity in subsurface aquifers receiving livestock wastewater input. Appl Env. Microbiol 66, 956–965. https://doi.org/10.1128/aem.66.3.956-965.2000

Colin, Y., Bouchali, R., Marjolet, L., Marti, R., Vautrin, F., Voisin, J., Bourgeois, E., Rodriguez-Nava, V., Blaha, D., Winiarski, T., Mermillod-Blondin, F., Cournoyer, B., 2020. Coalescence of bacterial groups originating from urban runoffs and artificial infiltration systems among aquifer microbiomes. Hydrol. Earth Syst. Sci. Discuss. 1–28. https://doi.org/10.5194/hess-2020-39

Datry, T., Malard, F., Gibert, J., 2005. Response of invertebrate assemblages to increased groundwater recharge rates in a phreatic aquifer. J. North Am. Benthol. Soc. 24, 461–477. https://doi.org/10.1899/04-140.1

Datry, T., Malard, F., Gibert, J., 2004. Dynamics of solutes and dissolved oxygen in shallow urban groundwater below a stormwater infiltration basin. Sci. Total Environ. 329, 215–229. https://doi.org/10.1016/j.scitotenv.2004.02.022

Datry, T., Malard, F., Vitry, L., Hervant, F., Gibert, J., 2003. Solute dynamics in the bed sediments of a stormwater infiltration basin. J. Hydrol. 273, 217–233. https://doi.org/10.1016/S0022-1694(02)00388-8

Escudié, F., Auer, L., Bernard, M., Mariadassou, M., Cauquil, L., Vidal, K., Maman, S., Hernandez-Raquet, G., Combes, S., Pascal, G., 2018. FROGS: Find, rapidly, OTUs with galaxy solution. Bioinformatics 34, 1287–1294. https://doi.org/10.1093/bioinformatics/btx791

Fandino, L.B., Riemann, L., Steward, G.F., Azam, F., 2005. Population dynamics of Cytophaga-Flavobacteria during marine phytoplankton blooms analyzed by real-time quantitative PCR. Aquat. Microb. Ecol. 40, 251–257. https://doi.org/10.3354/ame040251

Fillinger, L., Zhou, Y., Kellermann, C., Griebler, C., 2019. Non-random processes determine the colonization of groundwater sediments by microbial communities in a pristine porous aquifer. Environ. Microbiol. 21, 327–342. https://doi.org/10.1111/1462-2920.14463

Findlay, S.E.G., Sinsabaugh, R.L., Sobczak, W.V., Hoostal, M., 2003. Metabolic and structural response of hyporheic microbial communities to variations in supply of dissolved organic matter. Limnol. Oceanogr. 48, 1608–1617. https://doi.org/10.4319/lo.2003.48.4.1608

Fletcher, T.D., Shuster, W., Hunt, W.F., Ashley, R., Butler, D., Arthur, S., Trowsdale, S., Barraud, S., Semadeni-Davies, A., Bertrand-Krajewski, J.-L., others, 2015. SUDS, LID, BMPs, WSUD and more–The evolution and application of terminology surrounding urban drainage. Urban Water J. 12, 525–542. https://doi.org/10.1080/1573062x.2014.916314

Flörke, M., Schneider, C., McDonald, R.I., 2018. Water competition between cities and agriculture driven by climate change and urban growth. Nat. Sustain. 1, 51–58. https://doi.org/10.1038/s41893-017-0006-8

Flynn, T.M., Sanford, R.A., Ryu, H., Bethke, C.M., Levine, A.D., Ashbolt, N.J., Santo Domingo, J.W., 2013. Functional microbial diversity explains groundwater chemistry in a pristine aquifer. BMC Microbiol. 13, 146. https://doi.org/10.1186/1471-2180-13-146

Fontvieille, D.A., Outaguerouine, A., Thevenot, D.R., 1992. Fluorescein diacetate hydrolysis as a measure of microbial activity in aquatic systems: Application to activated sludges. Environ. Technol. 13, 531–540. https://doi.org/10.1080/09593339209385181

Foulquier, A., Malard, F., Barraud, S., Gibert, J., 2009. Thermal influence of urban groundwater recharge from stormwater infiltration basins. Hydrol. Process. 23, 1701–1713. https://doi.org/10.1002/hyp.7305

Foulquier, A., Malard, F., Mermillod-Blondin, F., Datry, T., Simon, L., Montuelle, B., Gibert, J., 2010. Vertical change in dissolved organic carbon and oxygen at the water table region of an aquifer recharged with stormwater: biological uptake or mixing? Biogeochemistry 99, 31–47. https://doi.org/10.1007/s10533-009-9388-7

Foulquier, A., Mermillod-Blondin, F., Malard, F., Gibert, J., 2011. Response of sediment biofilm to increased dissolved organic carbon supply in groundwater artificially recharged with stormwater. J. Soils Sediments 11, 382–393. https://doi.org/10.1007/s11368-010-0323-2

Freimann, R., Bürgmann, H., Findlay, S.E., Robinson, C.T., 2015. Hydrologic linkages drive spatial structuring of bacterial assemblages and functioning in alpine floodplains. Front. Microbiol. 6, 1221. https://doi.org/10.3389/fmicb.2015.01221

Fritch, T.G., McKnight, C.L., Yelderman Jr, J.C., Arnold, J.G., 2000. An aquifer vulnerability assessment of the Paluxy aquifer, central Texas, USA, using GIS and a modified DRASTIC approach. Environ. Manage. 25, 337–345. https://doi.org/10.1007/s002679910026

Goldscheider, N., Hunkeler, D., Rossi, P., 2006. Microbial biocenoses in pristine aquifers and an assessment of investigative methods. Hydrogeol. J. 14, 926–941. https://doi.org/10.1007/s10040-005-0009-9

Gouy, M., Guindon, S., Gascuel, O., 2010. SeaView Version 4: A multiplatform graphical user interface for sequence alignment and phylogenetic tree building. Mol. Biol. Evol. 27, 221–224. https://doi.org/10.1093/molbev/msp259

Griebler, C., Avramov, M., 2015. Groundwater ecosystem services: a review. Freshw. Sci. 34, 355–367. https://doi.org/10.1086/679903

Grösbacher, M., Eckert, D., Cirpka, O.A., Griebler, C., 2018. Contaminant concentration versus flow velocity: drivers of biodegradation and microbial growth in groundwater model systems. Biodegradation 29, 211–232. https://doi.org/10.1007/s10532-018-9824-2

He, Z., Ning, Z., Yang, M., Huang, G., Cui, H., Wang, H., Sun, J., 2019. The characterization of microbial communities response to shallow groundwater contamination in typical Piedmont region of Taihang Mountains in the north China Plain. Water 11, 736. https://doi.org/10.3390/w11040736

Heibl, C., 2008. Interfaces to Phylogenetic Software in R

Her, N., Amy, G., McKnight, D., Sohn, J., Yoon, Y., 2003. Characterization of DOM as a function of MW by fluorescence EEM and HPLC-SEC using UVA, DOC, and fluorescence detection. Water Res. 37, 4295–4303. https://doi.org/10.1016/S0043-1354(03)00317-8

Herzyk, A., Fillinger, L., Larentis, M., Qiu, S., Maloszewski, P., Hünniger, M., Schmidt, S.I., Stumpp, C., Marozava, S., Knappett, P.S.K., Elsner, M., Meckenstock, R., Lueders, T., Griebler, C., 2017. Response and recovery of a pristine groundwater ecosystem impacted by

toluene contamination – A meso-scale indoor aquifer experiment. J. Contam. Hydrol. 207, 17–30. https://doi.org/10.1016/j.jconhyd.2017.10.004

Hofmann, R., Griebler, C., 2018. DOM and bacterial growth efficiency in oligotrophic groundwater: absence of priming and co-limitation by organic carbon and phosphorus. Aquat. Microb. Ecol. 81, 55–71. https://doi.org/10.3354/ame01862

Houri-Davignon, C., Relexans, J.C., Etcheber, H., 1989. Measurement of actual electron transport system (ETS) activity in marine sediments by incubation with INT. Environ. Technol. Lett. 10, 91–100. https://doi.org/10.1080/09593338909384722

Kembel, S.W., Kembel, M.S.W., 2019. Package 'picante.'

Konrad, C.P., 2003. Effects of urban development on floods. US Geological Survey Tacoma. https://pubs.usgs.gov/fs/fs07603/

Kumar, A., Kaur, G., Kumar Singh, N., Mathan Kumar, R., Mayilraj, S., Bajaj, A., Kaur, N., Manickam, N., 2015. Taxonomic description and genome sequence of Rheinheimera mesophila sp. nov., isolated from an industrial waste site. Int. J. Syst. Evol. Microbiol. 65, 3666–3673. https://doi.org/10.1099/ijsem.0.000471

Landa, M., Cottrell, M.T., Kirchman, D.L., Blain, S., Obernosterer, I., 2013. Changes in bacterial diversity in response to dissolved organic matter supply in a continuous culture experiment. Aquat. Microb. Ecol. 69, 157–168. https://doi.org/10.3354/ame01632

Li, D., Alidina, M., Ouf, M., Sharp, J.O., Saikaly, P., Drewes, J.E., 2013. Microbial community evolution during simulated managed aquifer recharge in response to different biodegradable dissolved organic carbon (BDOC) concentrations. Water Res. 47, 2421–2430. https://doi.org/10.1016/j.watres.2013.02.012

Li, D., Sharp, J.O., Saikaly, P.E., Ali, S., Alidina, M., Alarawi, M.S., Keller, S., Hoppe-Jones, C., Drewes, J.E., 2012. Dissolved organic carbon influences microbial community composition and diversity in managed aquifer recharge systems. Appl. Environ. Microbiol. 78, 6819–6828. https://doi.org/10.1128/AEM.01223-12

Liu, Y., Lin, Y.-M., Yang, S.-F., Tay, J.-H., 2003. A balanced model for biofilms developed at different growth and detachment forces. Process Biochem. 38, 1761–1765. https://doi.org/10.1016/S0032-9592(02)00260-1

Liu, Y., Tay, J.-H., 2001. Metabolic response of biofilm to shear stress in fixed-film culture. J. Appl. Microbiol. 90, 337–342. https://doi.org/10.1046/j.1365-2672.2001.01244.x

Lozupone, C., Knight, R., 2005. UniFrac: A new phylogenetic method for comparing microbial communities. Appl. Environ. Microbiol. 71, 8228–8235. https://doi.org/10.1128/AEM.71.12.8228-8235.2005

Maes, P.W., Rodrigues, P.A.P., Oliver, R., Mott, B.M., Anderson, K.E., 2016. Diet-related gut bacterial dysbiosis correlates with impaired development, increased mortality and Nosema disease in the honeybee (Apis mellifera). Mol. Ecol. 25, 5439–5450. https://doi.org/10.1111/mec.13862

Mahé, F., Rognes, T., Quince, C., de Vargas, C., Dunthorn, M., 2014. Swarm: robust and fast clustering method for amplicon-based studies. PeerJ 2, e593. https://doi.org/10.7717/peerj.593

Marti, R., Ribun, S., Aubin, J.-B., Colinon, C., Petit, S., Marjolet, L., Gourmelon, M., Schmitt, L., Breil, P., Cottet, M., others, 2017. Human-driven microbiological contamination of benthic and hyporheic sediments of an intermittent peri-urban river assessed from MST and 16S rRNA genetic structure analyses. Front. Microbiol. 8, 19. https://doi.org/10.3389/fmicb.2017.00019

McMurdie, P.J., Holmes, S., 2013. Phyloseq: an R package for reproducible interactive analysis and graphics of microbiome census data. PloS One 8. https://doi.org/10.1371/journal.pone.0061217

Mentzer, J.L., Goodman, R.M., Balser, T.C., 2006. Microbial response over time to hydrologic and fertilization treatments in a simulated wet prairie. Plant Soil 284, 85–100. https://doi.org/10.1007/s11104-006-0032-1

Mermillod-Blondin, F., Foulquier, A., Maazouzi, C., Navel, S., Negrutiu, Y., Vienney, A., Simon, L., Marmonier, P., 2013. Ecological assessment of groundwater trophic status by using artificial substrates to monitor biofilm growth and activity. Ecol. Indic. 25, 230–238. https://doi.org/10.1016/j.ecolind.2012.09.026

Mermillod-Blondin, F., Voisin, J., Marjolet, L., Marmonier, P., Cournoyer, B., 2019. Clay beads as artificial trapping matrices for monitoring bacterial distribution among urban stormwater infiltration systems and their connected aquifers. Environ. Monit. Assess. 191, 58. https://doi.org/10.1007/s10661-019-7190-0.

Miura, T., Yamazoe, A., Ito, M., Ohji, S., Hosoyama, A., Takahata, Y., Fujita, N., 2015. The impact of injections of different nutrients on the bacterial community and its dechlorination activity in chloroethene-contaminated groundwater. Microbes Environ. 30, 164–171. https://doi.org/10.1264/jsme2.ME14127

Moorhead, D.L., Rinkes, Z.L., Sinsabaugh, R.L., Weintraub, M.N., 2013. Dynamic relationships between microbial biomass, respiration, inorganic nutrients and enzyme activities: informing enzyme-based decomposition models. Front. Microbiol. 4, 223. https://doi.org/10.3389/fmicb.2013.00223

Muscarella, M. E., Boot, C. M., Broeckling, C. D., & Lennon, J. T. (2019). Resource heterogeneity structures aquatic bacterial communities. ISME J. 13, 2183-2195.

Natarajan, P., Davis, A.P., 2015. Hydrologic performance of a transitioned infiltration basin managing highway runoff. J. Sustain. Water Built Environ. 1, 04015002. https://doi.org/10.1061/JSWBAY.0000797

Nogaro, G., Mermillod-Blondin, F., Montuelle, B., Boisson, J.-C., Bedell, J.-P., Ohannessian, A., Volat, B., Gibert, J., 2007. Influence of a stormwater sediment deposit on microbial and biogeochemical processes in infiltration porous media. Sci. Total Environ. 377, 334–348. https://doi.org/10.1016/j.scitotenv.2007.01.093

Pabich, W.J., Valiela, I., Hemond, H.F., 2001. Relationship between DOC concentration and vadose zone thickness and depth below water table in groundwater of Cape Cod, USA. Biogeochemistry 55, 247–268. https://doi.org/10.1023/a:1011842918260

Paradis, E., Schliep, K., 2019. ape 5.0: an environment for modern phylogenetics and evolutionary analyses in R. Bioinformatics 35, 526–528. https://doi.org/10.1093/bioinformatics/bty633

Peterson, G.L., 1977. A simplification of the protein assay method of Lowry et al. which is more generally applicable. Anal. Biochem. 83, 346–356. https://doi.org/10.1016/0003-2697(77)90043-4

Pitt, R., Clark, S., Field, R., 1999. Groundwater contamination potential from stormwater infiltration practices. Urban Water 1, 217–236. https://doi.org/10.1016/S1462-0758(99)00014-X

Quast, C., Pruesse, E., Yilmaz, P., Gerken, J., Schweer, T., Yarza, P., Peplies, J., Glöckner, F.O., 2012. The SILVA ribosomal RNA gene database project: improved data processing and web-based tools. Nucleic Acids Res. 41, D590–D596. https://doi.org/10.1093/nar/gks1219

R Core Team., 2018. R: A language and environment for statistical computing. R Foundation for Statistical Computing, Vienna, Austria. URL https://www.R-project.org/.

Rauch-Williams, T., Drewes, J.E., 2006. Using soil biomass as an indicator for the biological removal of effluent-derived organic carbon during soil infiltration. Water Res. 40, 961–968. https://doi.org/10.1016/j.watres.2006.01.007

Rinkes, Z.L., Sinsabaugh, R.L., Moorhead, D.L., Grandy, A.S., Weintraub, M.N., 2013. Field and lab conditions alter microbial enzyme and biomass dynamics driving decomposition of the same leaf litter. Front. Microbiol. 4, 260. https://doi.org/10.3389/fmicb.2013.00260

Schliep, K.P., 2011. phangorn: phylogenetic analysis in R. Bioinformatics 27, 592–593. https://doi.org/10.1093/bioinformatics/btq706

Seitzinger, S.P., Hartnett, H., Lauck, R., Mazurek, M., Minegishi, T., Spyres, G., Styles, R., 2005. Molecular-level chemical characterization and bioavailability of dissolved organic matter in stream water using electrospray-ionization mass spectrometry. Limnol. Oceanogr. 50, 1–12. https://doi.org/10.4319/lo.2005.50.1.0001

Smith, H.J., Zelaya, A.J., De León, K.B., Chakraborty, R., Elias, D.A., Hazen, T.C., Arkin, A.P., Cunningham, A.B., Fields, M.W., 2018. Impact of hydrologic boundaries on microbial planktonic and biofilm communities in shallow terrestrial subsurface environments. FEMS Microbiol. Ecol. 94, fiy191. https://doi.org/10.1093/femsec/fiy191

Smith, M., Cross, K., Paden, M., Laban, P., 2016. Spring–managing groundwater sustainably. IUCN Gland Switz. https://doi.org/10.2305/IUCN.CH.2016.WANI.8.en

Starr, R.C., Gillham, R.W., 1993. Denitrification and organic carbon availability in two aquifers. Groundwater 31, 934–947. https://doi.org/10.1111/j.1745-6584.1993.tb00867.x

Van der Gun, J., 2012. Groundwater and global change: trends, opportunities, and challenges. The United Nations world water assessment program –ISBN : 978-92-3-001049-2

Voisin, J., Cournoyer, B., Marjolet, L., Vienney, A., Mermillod-Blondin, F., 2020. Ecological assessment of groundwater ecosystems disturbed by recharge systems using organic matter quality, biofilm characteristics, and bacterial diversity. Environ. Sci. Pollut. Res. Int. 27, 3295–3308. https://doi.org/10.1007/s11356-019-06971-5

Voisin, J., Cournoyer, B., Mermillod-Blondin, F., 2016. Assessment of artificial substrates for evaluating groundwater microbial quality. Ecol. Indic. 71, 577–586. https://doi.org/10.1016/j.ecolind.2016.07.035

Voisin, J., Cournoyer, B., Vienney, A., Mermillod-Blondin, F., 2018. Aquifer recharge with stormwater runoff in urban areas: Influence of vadose zone thickness on nutrient and bacterial transfers from the surface of infiltration basins to groundwater. Sci. Total Environ. 637–638, 1496–1507. https://doi.org/10.1016/j.scitotenv.2018.05.094

Williamson, W.M., Close, M.E., Leonard, M.M., Webber, J.B., Lin, S., 2012. Groundwater biofilm dynamics grown in situ along a nutrient gradient. Ground Water 50, 690–703. https://doi.org/10.1111/j.1745-6584.2011.00904.x

Winderl, C., Schaefer, S., Lueders, T., 2007. Detection of anaerobic toluene and hydrocarbon degraders in contaminated aquifers using benzylsuccinate synthase (bssA) genes as a functional marker. Environ. Microbiol. 9, 1035–1046. https://doi.org/10.1111/j.1462-2920.2006.01230.x

Wright ES (2016). Using DECIPHER v2.0 to analyze big biological sequence data in R. The R Journal 8, 352-359.

Zhou, Y., Kellermann, C., Griebler, C., 2012. Spatio-temporal patterns of microbial communities in a hydrologically dynamic pristine aquifer. FEMS Microbiol. Ecol. 81, 230–242. https://doi.org/10.1111/j.1574-6941.2012.01371.x

Table 1. Main characteristics of the Stormwater Infiltration Systems (SIS)

SIS	Vadose zone thickness (m)	Infiltration surface (ha)	Catchment area (ha)	Surroundings areas
Grange Blanche (GB)	1.0	0.32	300	Intensive cultures (corn and wheat), small houses and roads
Minerve (MIN)	2.0	0.42	165	Urban land use (commercial centers, lawns and large roads), fire station
IUT (IUT)	2.5	0.09	2.5	Teaching and research buildings, parking lots, roads and lawns

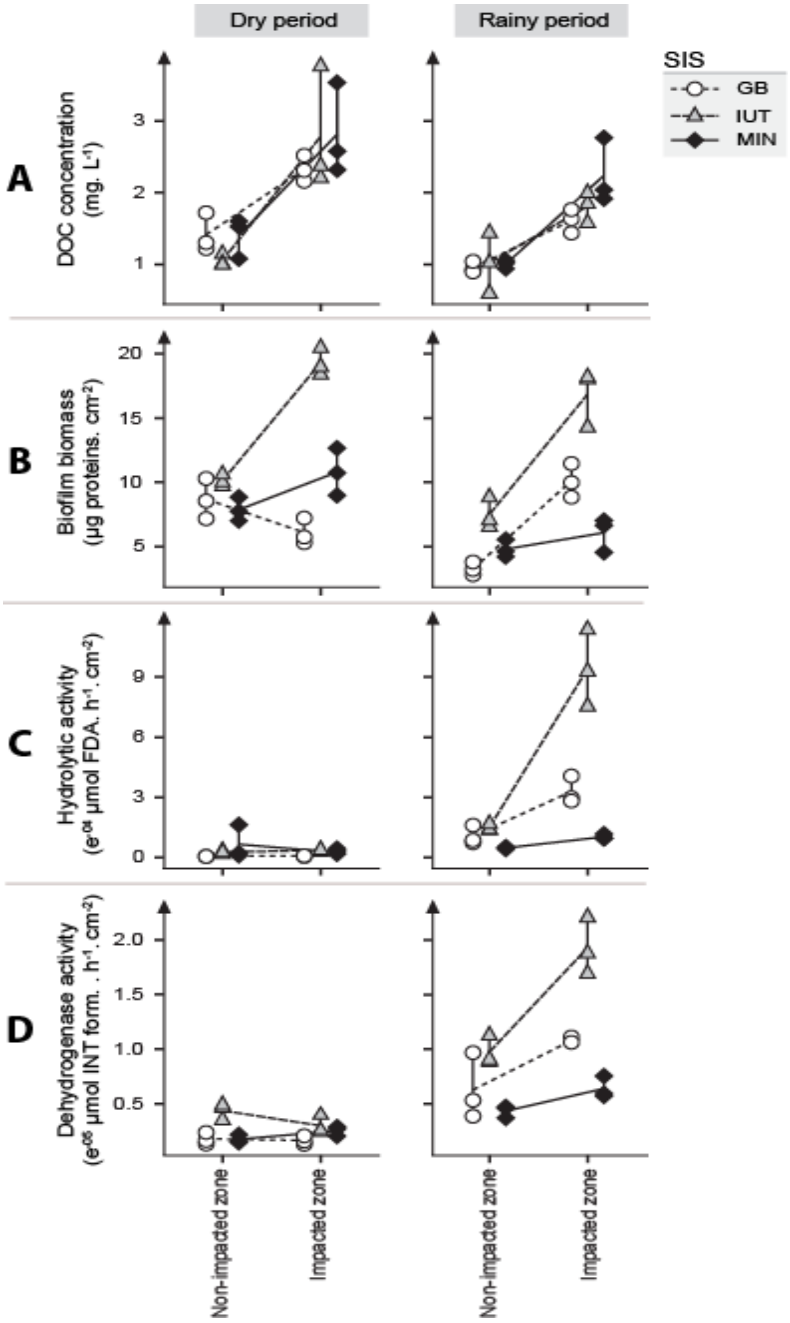

Fig. 1. Groundwater dissolved organic carbon concentration (mg. L^{-1}), and biofilm biomass (µg protein. cm^{-2}), hydrolytic activities (10^{-4} µmol FDA hydrolyzed. h^{-1}. cm^{-2}) and dehydrogenase activities (10^{-5} µmol INT formazan produced. h^{-1}. cm^{-2}) measured on non-SIS-impacted and SIS-impacted zones (left and right within each individual panel, respectively) of the three stormwater infiltration systems - SIS (Grange-Blanche –GB, white circles; IUT, grey triangles; Minerve-MIN, black diamonds) during the dry and the rainy periods (left and right panels, respectively).

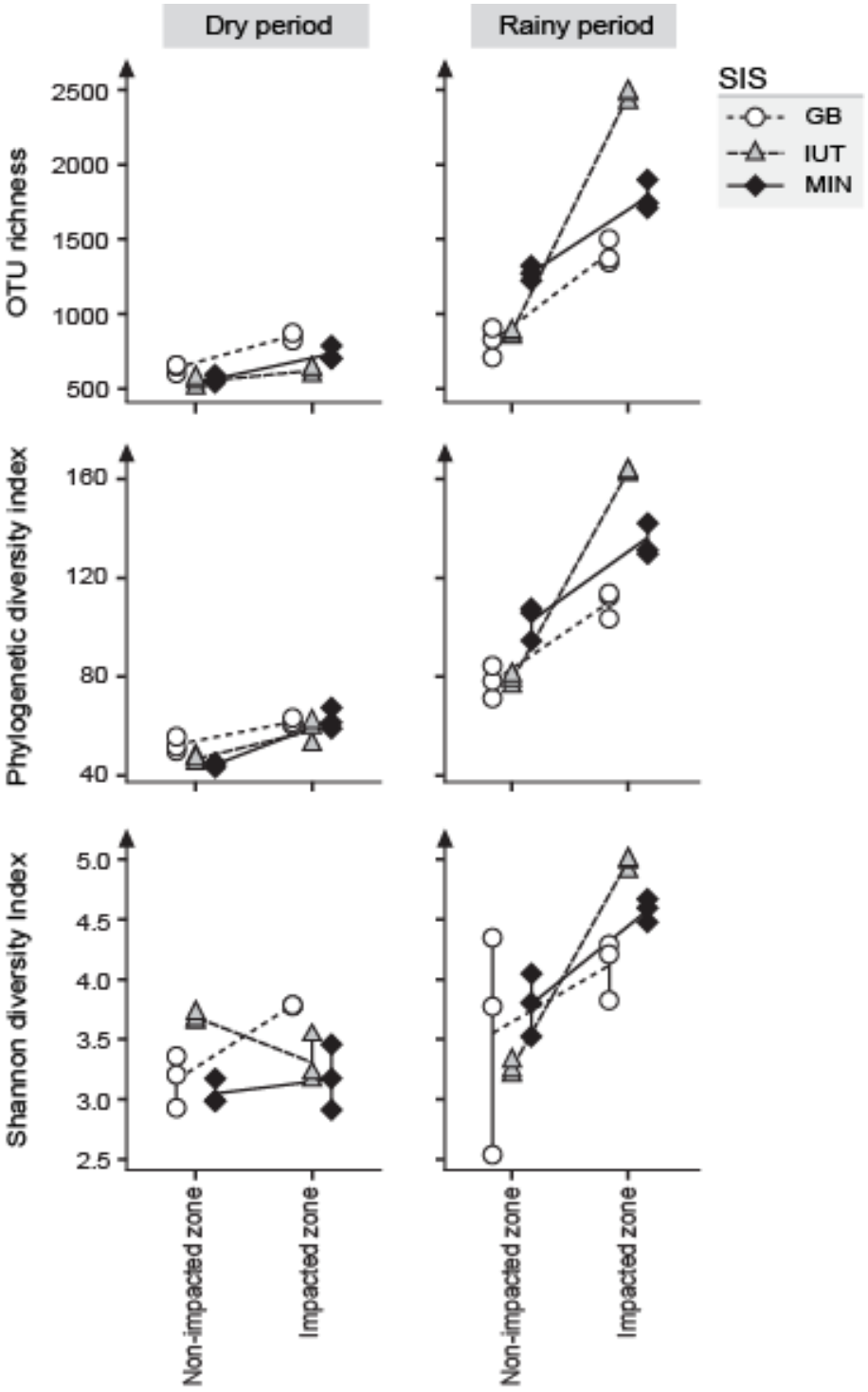

Fig. 2. Aquifer biofilms metabarcoding 16S rRNA V5-V7 genetic diversity analyses. OTUs richness (top panels), Faith's phylogenetic diversity (middle panels) and Shannon diversity (bottom panels) indices measured on non-SIS-impacted and SIS-impacted zones (left and right of each individual panel, respectively) of the three stormwater infiltration systems SIS (Grange-Blanche –GB, white circles; IUT, gray triangles; Minerve-MIN, black diamonds) during the dry and the rainy periods (left and right panels, respectively).

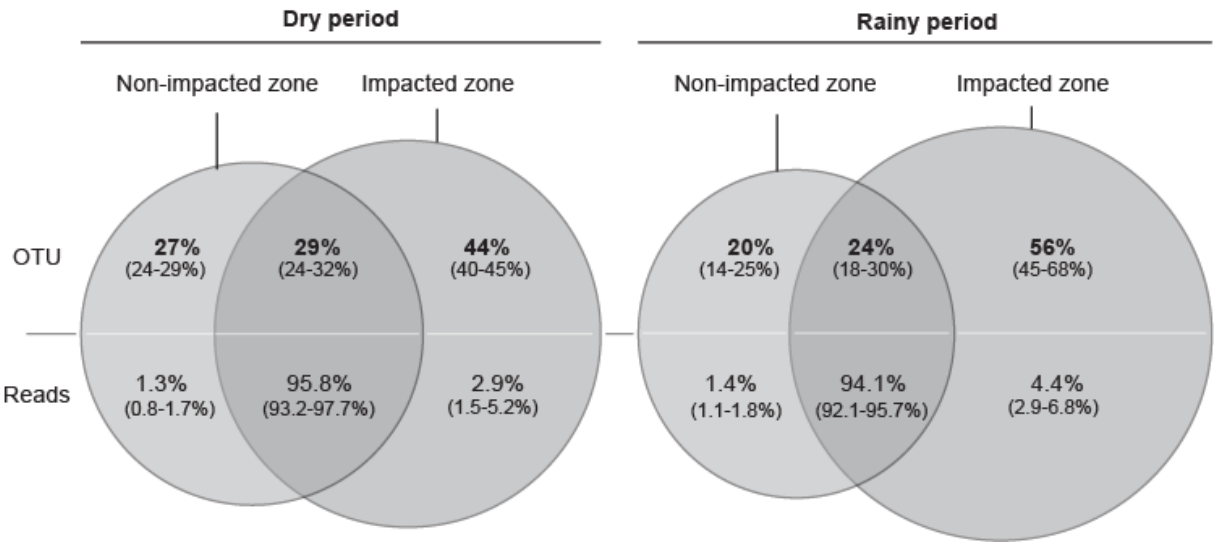

Fig. 3. Venn diagrams representing the distribution of OTUs recovered from biofilms during the dry and rainy periods (left and right diagrams, respectively). Distribution is presented as the percentage of the whole OTUs pool (for each SIS and each period) being detected i) only in non-SIS-impacted zone (left of each diagram), ii) only in SIS-impacted zone (right of each panel) and iii) on both zones (shared OTUs; dark-gray overlap area). Based on read number for each OTUs, we indicate the corresponding distribution of reads within SIS (also as a percentage of the total read numbers for each period and SIS) on the bottom part of each diagram. The main percentages in bold represent the average numbers over the three SIS and the percentages in square brackets correspond to the range.

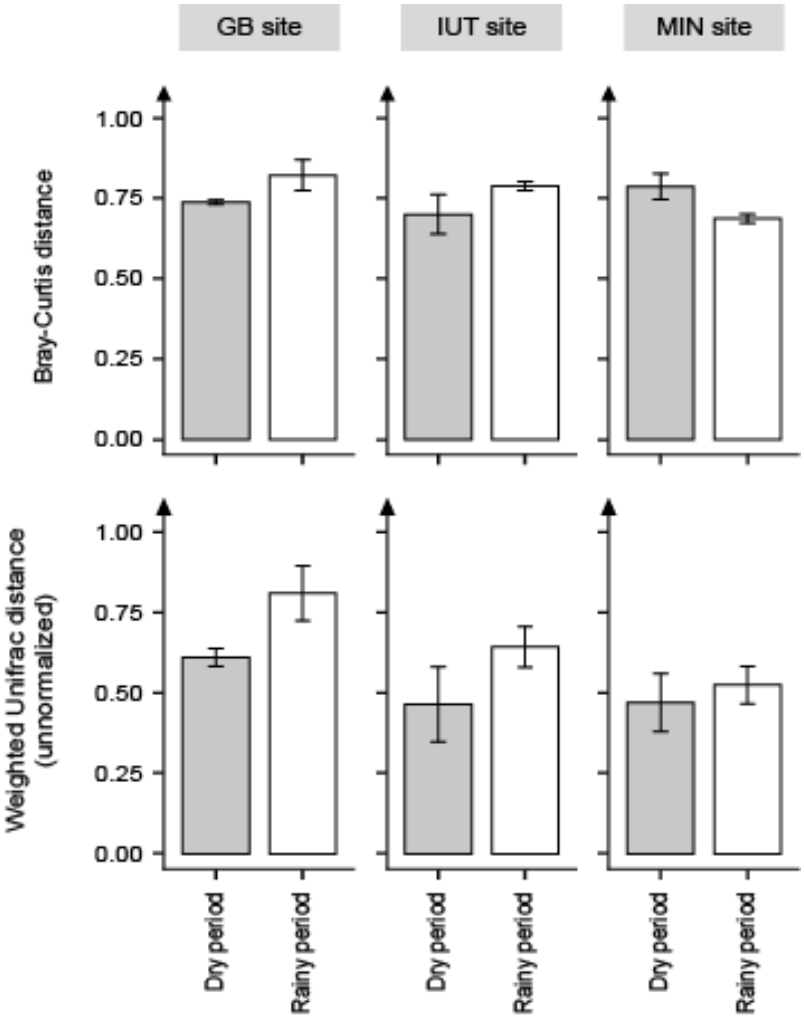

Fig. 4. Aquifer biofilm metabarcoding 16S rRNA V5-V7 beta diversity analyses. Bray-Curtis and unnormalized weighted Unifrac distances (top and bottom panels, respectively) calculated between the non-SIS-impacted and the SIS-impacted zones, for each SIS (Grange-Blanche – GB, left panels; IUT, middle panels; Minerve-MIN, right panels) during the dry (gray) and the rainy (white) periods. (see 2.4.3 for details).

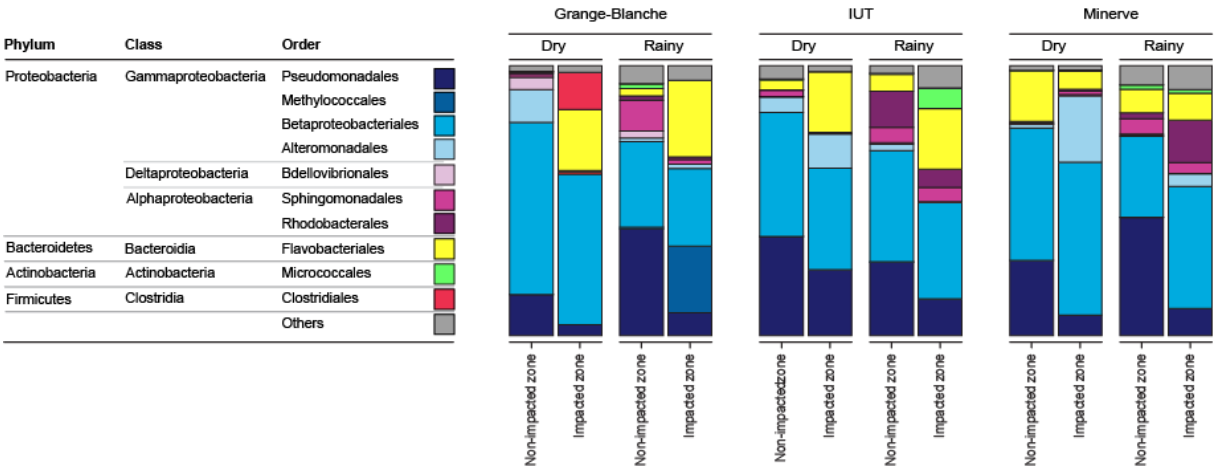

Fig. 5. Bacterial taxa in aquifer biofilms inferred from metabarcoding 16S rRNA V5-V7 gene reads. Relative abundance (mean of three replicates per condition) of the ten most represented bacterial orders during the dry and the rainy periods for each of the three SIS. Sequences not assigned to one of these orders are pooled in “Others”.